Published in final edited form as:
J Biol Chem. 2003 September 26; 278(39): 37032–37040. doi:10.1074/jbc.M304316200.

Oxidized Lipoproteins Inhibit Surfactant Phosphatidylcholine Synthesis via Calpain-mediated Cleavage of CTP:Phosphocholine Cytidylyltransferase*

Jiming Zhou[‡], **Alan J. Ryan**[‡,§], **Jheem Medh**[‡], and **Rama K. Mallampalli**[‡,§,¶,‖]

[‡]Department of Internal Medicine, The University of Iowa College of Medicine, Iowa City, Iowa 52242

[¶]Department of Biochemistry, The University of Iowa College of Medicine, Iowa City, Iowa 52242

[§]Department of Veterans Affairs Medical Center, The University of Iowa College of Medicine, Iowa City, Iowa 52242

Abstract

We investigated effects of pro-atherogenic oxidized lipoproteins on phosphatidylcholine (PtdCho) biosynthesis in murine lung epithelial cells (MLE-12). Cells surface-bound, internalized, and degraded oxidized low density lipoproteins (Ox-LDL). Ox-LDL significantly reduced [^{3}H]choline incorporation into PtdCho in cells by selectively inhibiting the activity of the rate-regulatory enzyme, CTP:phosphocholine cytdylyltransferase (CCT). Ox-LDL coordinately increased the cellular turnover of CCTα protein as determined by [^{35}S]methionine pulse-chase studies by inducing the calcium-activated proteinase, calpain. Forced expression of calpain or exposure of cells to the calcium ionophore, A23187, increased CCTα degradation, whereas overexpression of the endogenous calpain inhibitor, calpastatin, attenuated Ox-LDL-induced CCTα degradation. The effects of Ox-LDL on CCTα breakdown were attenuated in calpain-deficient cells. *In vitro* calpain digestion of CCTα isolated from cells transfected with truncated or internal deletion mutants indicated multiple cleavage sites within the CCTα primary structure, leading to the generation of a 26-kDa (p26) fragment. Calpain hydrolysis of purified CCTα generated p26, which upon NH_2-terminal sequencing localized a calpain attack site within the CCTα amino terminus. Expression of a CCTα mutant where the amino-terminal cleavage site and a putative carboxyl-terminal hydrolysis region were modified resulted in an enzyme that was significantly less sensitive to proteolytic cleavage and restored the ability of cells to synthesize surfactant PtdCho after Ox-LDL treatment. Thus, these results provide a critical link between proatherogenic lipoproteins and their metabolic target, CCTα, resulting in impaired surfactant metabolism.

Phosphatidylcholine (PtdCho)[1] has diverse biologic roles in mammalian cells and serves as the major phospholipid of pulmonary alveolar surfactant. Surfactant is synthesized and secreted from alveolar type II epithelial cells in a lipoproteinaceous form highly enriched with

*This study was supported by a Merit Review Award from the Office of Research and Development, Department of Veterans Affairs, and National Institutes of Health R01 Grants HL55584, HL68135, and HL71040 (to R. K. M.).

‖To whom correspondence should be addressed: Division of Pulmonary Diseases, Critical Care, and Occupational Medicine, Dept. of Internal Medicine, University of Iowa College of Medicine, Iowa City, IA 52242. Tel.: 319-356-1265; Fax: 319-353-6406; ramamallampalli@uiowa.edu.

[1]The abbreviations used are: PtdCho, phosphatidylcholine; CCT, CTP:phosphocholine cytidylyltransferase; LDL, low density lipoprotein; Ox-LDL, oxidized low density lipoproteins; VLDL, very low density lipoprotein; Ox-VLDL, oxidized very low density lipoproteins; LPDS, lipoprotein-deficient serum; MLE-12, murine lung epithelia; CHO, Chinese hamster ovary; CDP-choline, cytidine diphosphocholine; DSPtd-Cho, disaturated phosphatidylcholine; ALLN, *N*-acetyl-Leu-Leu-Nle-CHO; LysoPtdCho, lysophosphatidylcholine; ANOVA, analysis of variance; MALDI-MS, matrix-assisted laser desorption ion mass spectrometry; CMV, cytomegalovirus.

disaturated phosphatidylcholine (DSPtdCho), a critical surface-active component (1). DSPtdCho biosynthesis requires the uptake of choline into alveolar type II epithelial cells with the subsequent entry of this metabolite into the CDP-choline pathway (2). A key step in this pathway involves the conversion of cholinephosphate to CDP-choline, which is catalyzed by the rate-limiting enzyme CTP: phosphocholine cytidylyltransferase (CCT) (EC 2.7.7.15 (2)).

CCT is an amphitropic enzyme, thus exhibiting interconversion between its soluble and membrane-associated forms. Accordingly, CCT localizes to several intracellular organelles, most notably the nuclear envelope and endoplasmic reticulum (3,4). CCT activity is largely controlled by association with membrane lipids, and lipid regulation is well documented (2). For example, anionic phospholipids, diacylglycerol, and unsaturated fatty acids all have been shown to potently activate the enzyme *in vitro* (5–7). CCT is also a phosphoenzyme, and membrane activation of CCT is influenced by enzyme phosphorylation status (5). In addition, CCT is controlled at the level of gene transcription and by altered mRNA and protein stability (8–12).

Three CCT isoforms exist in cells: CCTα, CCTβ1, and CCTβ2 (13). CCTα, the predominant species in alveolar epithelia contains four distinct functional domains including an amino-terminal nuclear localization domain, a mid-portion catalytic sequence, a lipid-binding domain, and a carboxyl-terminal phosphorylation domain. A second lipid-interacting domain within the carboxyl terminus of CCTα has been identified recently (14). All CCT isoforms are catalytically active and are regulated by the availability of exogenous lipids.

Studies in our laboratory have demonstrated that circulating native lipoproteins provide an important source of regulatory lipids for CCT activation and surfactant PtdCho synthesis (15,16). Very low density lipoproteins (VLDL) stimulate CCT activity and DSPtdCho synthesis *in vivo* (16). However, all lipoproteins deteriorate through an oxidative process, and lipoprotein oxidation is of central importance in the pathogenesis of atherosclerotic heart disease (17). Low density lipoproteins (LDL) oxidize in the arterial intima in the presence of transition metals, thereby stimulating leukocyte-endothelial adhesion and recruitment of macrophages via chemoattractants. Severely oxidized LDL (Ox-LDL) is no longer recognized by the classic LDL receptor pathway, which is subject to feedback inhibition by intracellular cholesterol content but is taken up by macrophages via scavenger receptors. This in turn leads to the generation of the foam cell and the evolution of the fatty streak, hallmarks of atherosclerosis.

Oxidized lipoproteins also appear to participate in the pathogenesis of several lung disorders such as asthma, acute lung injury, and cystic fibrosis (18). Many of these disorders are characterized by decreased levels of surfactant PtdCho (19). For example, in acute lung injury there is leakage of native lipoproteins from serum into the alveolar space (20). These native lipoproteins are modified by an oxidative stress, intrinsic to lung injury, resulting from impaired antioxidant defenses, the presence of reactive oxidant species, and exposure to hyperoxia during mechanical ventilation (20). Thus, pulmonary oxidative modification of native lipoproteins may be a critical event leading to altered surfactant lipid composition. Interestingly, alveolar type II epithelial cells express scavenger receptors that mediate uptake of antioxidants (21). Collectively, these observations led us to hypothesize that Ox-LDL catabolism by alveolar epithelia might down-regulate surfactant DSPtdCho biosynthesis. To test this hypothesis, we determined the effects of oxidized lipoproteins on a key regulatory step within the CDP-choline pathway. We observed that these modified lipoproteins inhibit PtdCho synthesis in alveolar epithelia by triggering CCTα degradation via calpain-mediated cleavage of the enzyme.

EXPERIMENTAL PROCEDURES

Materials

VLDL and LDL were purchased from Intracel (Frederick, MD). Lipoprotein-deficient serum (LPDS) ($d > 1.21$ g/ml) was isolated by ultracentrifugation (22). The MLE-12 and CHO cell lines were purchased from American Type Culture Collection (Manassas, VA). Radio-labeled lipoproteins were prepared as described (15). Lactacystin, A23187, *N*-acetyl-Leu-Leu-Nle-CHO (ALLN), recombinant rat calpain II, and calpastatin were purchased from Calbiochem (La Jolla, CA). A rabbit polyclonal CCTα antibody to synthetic peptide (10) was generated by Covance Research Products Inc. (Richmond, CA), and rabbit polyclonal antibodies to M- and μ-calpain were from ABR-Affinity BioReagents (Golden, CO). The X-blue cells were from Stratagene (La Jolla, CA). The *Taq*man reverse transcription reagents, SYBR Green PCR master mix, and ProBlot were from Applied Biosystems (Foster City, CA). The pCR-TOPO4 plasmids and *Escherichia coli* Top10 competent cells were obtained from Invitrogen (Carlsbad, CA), and FuGENE6 transfection reagent was purchased from Roche Diagnostics. The Geneclean2 Kit was obtained from Bio101 (Carlsbad, CA). Recombinant histidine-tagged CCTα was kindly provided by Dr. Suzy Jackowski (23). The plasmids pCMV5-CCT_{236} and pCMV5-CCT_{314} were kindly provided by Dr. Claudia Kent (24). The pOP13-JHCPIS (calpastatin-inhibitory domain fragment) plasmid was a gift from Dr. Neil Forsberg (25). Calpain-deficient (Capn −/−) and wild-type (Capn +/+) embryonic fibroblasts were kindly provided by Dr. Peter Greer (26). The QuikChange site-directed mutagenesis kit was from Stratagene. The Advantage cDNA polymerase and the SMART™ cDNA library construction kit were from Clontech, (Palo Alto, CA). All DNA sequencing was performed by the University of Iowa DNA core facility. M-PER mammalian protein extraction reagent and the B-PER 6XHis spin purification kits were obtained from Pierce. NH_2-terminal sequencing was performed by the Protein Core Laboratory at Michigan State University (East Lansing, MI).

Lipoprotein Oxidation

Lipoproteins were oxidized by dialysis in phosphate-buffered saline containing 5 μM $CuSO_4$ for 24 h at 37 °C (27). Confirmation of lipoprotein oxidization was by the malonaldehyde assay and by apoprotein B-100 immunoblotting.

Cell Isolation and Culture

Primary rat type II epithelial cells were isolated as described (28). Cells were cultured in Dulbecco's minimum essential medium containing 10% LPDS for up to 24 h. MLE cells were cultured in Hite's medium containing LPDS for up to 48 h with or without LDL (100 μg/ml), Ox-LDL (10–100 μg/ml), or Ox-VLDL (10–100 μg/ml) (29). In some studies, cells were preincubated with lactacystin (5 μM) or ALLN (40 μg/ml) for 1 h prior to exposure of cells to Ox-LDL. Cells lysates were isolated after brief sonication in Buffer A (10) at 4 °C prior to analysis.

Cell Surface Binding, Internalization, and Degradation of Oxidized Lipoproteins

Cellular catabolism of lipoproteins was determined as described (15). Surface binding and internalization were defined as radioactivity that was released or remained cell-associated, respectively, following incubation of cells at 4 °C in buffer containing 10 mg/ml tripolyphosphate. Degradation was defined as the trichloroacetic acid-soluble radioactivity in the medium.

PtdCho and DSPtdCho Analysis

Cells were pulsed with 1 μCi of [*methyl*-^{3}H]choline chloride during the final 2 h of incubation with or without lipoproteins. Total cellular lipids were extracted (30) and spotted on LK5D

plates, and PtdCho was resolved using thin layer chromatography (10). DSPtdCho determination was as described (31).

Enzyme Assays

CCT activity was determined by measuring the rate of incorporation of [*methyl*-^{14}C] phosphocholine into CDP-choline using a charcoal extraction method (32).

Immunoblot Analysis

Equal amounts of total protein from cell lysates, adjusted to give a final concentration of 60 mM Tris-HCl, pH 6.8, 2% SDS, 10% glycerol, 0.1% bromphenol blue, and 5% β-mercaptoethanol, were heated at 100 °C for 5 min. Samples were then electrophoresed through a 10% SDS-polyacrylamide gel and transferred to a nitrocellulose membrane. Immunoreactive CCTα and calpain were detected using the ECL Western blotting detection system. The dilution factors for all polyclonal antibodies were 1:1000.

[^{35}S]Methionine Pulse-Chase and CCTα Immunoprecipitation

Turnover of CCTα was determined by preincubating MLE cells for 1 h in methionine-deficient medium and then pulsing with [^{35}S]methionine (60 μCi/ml) for 4 h at 37 °C (10). Cells were rinsed twice in a similar medium and chased with serum-free Hite's medium containing 10 mM methionine and 3 mM cysteine for 0–24 h, with or without Ox-LDL. Cells were harvested and CCTα immunoprecipitated using the CCTα polyclonal antibody prior to separation using SDS-PAGE (10).

Cloning of Rat CCTα

Total cellular RNA was isolated from primary rat adult type II alveolar epithelial cells using Tri-Reagent per the manufacturer's instructions. Double-stranded cDNA was generated from RNA using the SMART™ cDNA library construction kit following the manufacturer's instructions. The cDNA encoding the open reading frame for CCTα was generated using double-stranded cDNA as a template and using the sense primer 5′-agatctatggatgcacagagttcag-3′ and antisense primer 5′-tctagattagtcctcttcatcctcgctg-3′ in a two-step PCR amplification using Advantage cDNA polymerase. The reaction conditions were as follows: 94 °C for 2 min; 94 °C for 30 s, 68 °C for 3 min, 18 cycles. The ~1100-bp CCTα open reading frame was purified using the Geneclean2 kit and cloned into pCR4-TOPO, and plasmid minipreps were verified by sequencing. This clone was then digested by *Bgl*II and *Xba*I, purified by Geneclean2, and ligated into a pCMV5 expression vector previously digested with the same restriction enzymes.

Construction of CCTα Mutants

An internal deletion CCTα mutant (termed CCTα$_{289}$), lacking the putative membrane-binding domain of CCTα (amino acid residues 240–290), was generated as follows. pCMV5-CCTα was used as a template for PCR using the sense primer 5′-ggagctcaatgtcagctttatcaacagtcccaagcacagtccc-3′ and antisense primer 5′-tctagattagtcctcttcatcctcgctg-3′ to generate a 230-bp fragment that was purified and directionally cloned into pCR4-TOPO for transformation into TOP10-competent cells. pCMV5-CCTα was digested by *Sac*I and *Xba*I, whereas pCR4-TOPO-CCTα was digested by *Bgl*II and *Sac*I, generating 234- and 687-bp fragments, respectively. These products were purified and ligated into the *Bgl*II/*Xba*I site in pCMV5 using T_4 ligase at 15 °C overnight.

An amino-terminal CCTα mutant (CCTα$_{SM}$), in which Ser^5-Ser^6 were mutated to Met^5-Met^6, was generated using the QuikChange site-directed mutagenesis kit. The oligonucleotides used were 5′-ctatggatgc acagatgatg gctaaagtca attcaagg-3′ (sense) and 5′-ccttgaattg actttagcca

tcatctgtgc atccatag-3′ (antisense), and pCMV5-CCT plasmid DNA was used as a template. PCR conditions were as follows: 95 °C for 30 s, 18 cycles at 95 °C for 30 s, 55 °C for 60 s, and 68 °C for 6 min.

We also generated a CCTα protein, termed $CCT\alpha_{Penta}$, that harbored the amino-terminal mutation above but also had residues Lys^{238}-Lys^{239}-Tyr^{240} mutated to Arg^{238}-Arg^{239}-Phe^{240}, using procedures similar to those described above. The oligonucleotides used were 5′-gct tta tca acg aaa gga gat tcc act tgc aag aac g-3′ (sense) and 5′-cgt tct tgc aag tgg aat ctc ctt tcg ttg ata aag c-3′ (antisense), with $CCT\alpha_{SM}$ plasmid DNA used as a template. The $CCT\alpha_{Penta}$ construct was verified by DNA sequencing.

Construction of Histidine-tagged CCTα and $CCT\alpha_{289}$ Expression Vectors

Carboxyl-terminal histidine-tagged full-length CCTα and the deletion mutant $CCT\alpha_{289}$ vectors were generated by PCR using pCMV5-CCTα or pCMV5-$CCT\alpha_{289}$ as templates with the sense primer 5′-agatctatggatgcacagagttcag-3′ and antisense primer 5-′ tctagatcaatgatgatgatgatgatggtcctcttcatcctcgc-3′. The resulting ~1100- and ~900-bp PCR products first were cloned into pCR4-TOPO and then ligated into the *Bgl*II and *Xba*I sites of pCMV5. The pCMV5-CCTα-His and pCMV5-$CCT\alpha_{289}$-His were verified by DNA sequencing.

Purification of Recombinant pCMV5-CCTα-His and $CCT\alpha_{289}$-His Proteins

The pCMV5-CCTα-His and $CCT\alpha_{289}$-His plasmids were transiently transfected into CHO cells. After 24 h, cell lysates were harvested using the M-PER mammalian protein extraction reagent. CCTα-histidine tag proteins were purified using the B-PER 6XHis spin purification kit following the manufacturer's instructions.

Construction of M-calpain by Site-directed Mutagenesis

Mutagenesis of the M-calpain expression vector (pOP13-JHMS (25)) was performed by using the QuikChange site-directed mutagenesis kit and the primers 5′-ggagcccttggggactgctggcttctggct-3′ and 5′-agccagaagccagcagtccccaagggctcc-3′. The PCR conditions were: 95 °C for 30 s, 18 cycles at 95 °C for 30 s, 55 °C for 60 s, and 68 °C for 9 min. The resulting pOP13-calpain was verified by DNA sequencing.

Real-time PCR Analysis

Total cellular RNA from MLE cells was obtained using Tri-Reagent. *Taq*man reverse transcription reagents were used to generate cDNA from cellular RNA. Real-time PCR was then performed on cDNA using the Applied Biosystems 7700 real-time PCR instrument and the SYBR Green PCR master mix. M-calpain mRNA detection primers were: 5′ primer, 5′-caagtcatcgttgcccgg-3′, and 3′ primer, 5′-ccaaacaccgcacaaaattg-3′. The μ-calpain 5′ primer was 5′-tcacccgctactcggagc-3′, and 3′ primer was 5′-cgcacaagacagcacacaaa-3′. *Taq*man rodent glyceraldehyde-3-phosphate dehydrogenase (GAPDH) control reagents were used as the internal control. Standard curves generated for calpain and compared with GAPDH using serial dilutions of mRNA were found to be linear from 0.08 ng to 50 ng RNA in the reaction mixture. This range included effective concentrations used in experiments.

Transient Transfection and Over-expression of Recombinant Proteins

Transfections were conducted for 120 min in 0% fetal bovine serum medium using 10 μl of FuGENE 6™ reagent and 5 μg/dish of the desired plasmid. Immediately after transfections, cells were transferred to medium containing 2–10% fetal bovine serum and allowed to recover for 24 h before cell lysates were harvested for analysis. In other studies, cells were transfected

with pOP13-JHCPIS (calpastatin inhibitory domain fragment) with or without Ox-LDL (100 μg/ml) for 48 h or with pOP13-calpain.

In Vitro Digestion of CCTα

Digestions were conducted at 35 °C for 20 min in 50-μl reaction mixtures containing 25 μg of purified rat CCTα-His and 0.7 μg of recombinant rat M-calpain in calpain buffer (20 mM Tris, pH 7.5, 2 mM dithiothreitol, 1% Tween 20, and 0.015% Triton X-100). The reaction was started by adding $CaCl_2$ to a final concentration of 3 mM and was terminated by adding 10 mM EDTA and then heating the samples to 95 °C. After digested proteins were resolved by SDS-PAGE, they were transferred to Problot membranes for Coomassie Blue staining and submitted to NH_2-terminal sequencing or processed for immunoblotting.

Statistical Analysis

Statistical analysis was performed using one-way ANOVA with a Bonferroni adjustment or Student's unpaired *t* test (33).

RESULTS

Oxidized Lipoprotein Catabolism by Alveolar Epithelia

MLE cells bound, internalized, and degraded ^{125}I-labeled oxidized human LDL and oxidized VLDL. Cells exhibited a nearly 8-, 4-, and 6-fold increase in steady-state uptake, internalization, and degradation of ^{125}I-Ox-LDL ligand, respectively (Fig. 1). Ox-LDL catabolism increased steadily up to concentrations of ~25 μg/ml ligand, thereafter reaching a plateau at higher doses indicative of saturable kinetics (Fig. 1). Cells also exhibited a dose-dependent increase in catabolism of Ox-VLDL; however, saturability was not always observed within the range of lipoproteins tested in these studies (Fig. 1, *insets*). In preliminary studies, primary rat alveolar type II epithelial cells also bound and internalized oxidized lipoproteins (data not shown). Thus, alveolar epithelia actively engage in modified lipoprotein catabolism.

Ox-LDL Inhibits Surfactant PtdCho Biosynthesis

Ox-LDL significantly decreased the incorporation of [*methyl*-^{3}H]choline into PtdCho and DSPtdCho in primary type II epithelia and MLE cells. In primary cells, Ox-LDL significantly decreased choline incorporation into PtdCho by ~40% after 24 h of exposure (Fig. 2*A*). Similar effects of Ox-LDL were observed on choline incorporation into DSPtdCho, the primary surface-active component of surfactant, which was reduced by 46% *versus* control (Fig 2*A*, *inset*). In MLE cells, the effects of Ox-LDL were more pronounced, as Ox-LDL inhibited choline incorporation into PtdCho and DSPtdCho by 75 and 67%, respectively (Fig. 2*B* and *inset*). To further investigate the effects of Ox-LDL on DSPtdCho synthesis, we assayed enzymes within the CDP-choline pathway. Ox-LDL produced a 43% decrease in CCT activity in primary cells (Fig. 2*C*) and a dose-dependent decrease in CCT activity in MLE cells (Fig. 2*C*, *inset*; $n = 3$, $p < 0.05$ *versus* control). In contrast, these particles tended to increase cholinephosphosphotransferase activity but did not alter choline kinase activity in primary cells (data not shown). Thus, Ox-LDL substantially reduces surfactant lipid biosynthesis by selectively inhibiting the rate-regulatory step within the CDP-choline pathway.

Ox-LDL Increases CCTα Protein Turnover

Ox-LDL produced a dose-dependent decrease in the steady-state levels of the 42-kDa native CCTα protein after 48 h of exposure without having any effect on β-actin (Fig. 3, *A* and *B*). Similar effects on CCTα levels were seen after Ox-VLDL treatment of MLE cells (Fig. 3*C*) and in primary alveolar cells (Fig. 3*D*). These data suggest that Ox-LDL decreases PtdCho synthesis by increasing CCTα protein degradation.

Confirmation of Ox-LDL effects on enzyme turnover was made using [^{35}S]methionine pulse-chase studies. The amount of [^{35}S]methionine incorporated into immunoprecipitable CCTα was determined after a 4-h pulse followed by a 0–24-h chase with unlabeled methionine conducted in the presence or absence of Ox-LDL. The amount of [^{35}S]methionine incorporated into immunoprecipitable CCTα was decreased at 6 h by Ox-LDL (Fig. 3*E*), and by 18–24 h substantially less CCTα was observed in Ox-LDL-treated cells compared with control.

Effects of Ox-LDL on CCTα Expression Are Mediated by Calpain

Cells were preincubated with ALLN and lactacystin, calpain, and 20 S proteasome inhibitors, respectively, and samples were analyzed for CCTα protein content and activity (Fig. 4, *A* and *B*). Pretreatment with either ALLN or lactacystin partly blocked Ox-LDL-induced CCTα degradation (Fig. 4*A*). The effects of ALLN were generally greater than lactacystin in antagonizing Ox-LDL on CCTα protein levels, although both inhibitors were equally effective in attenuating the lipoprotein-induced inhibition of CCT activity (Fig. 4, *A* and *B*). To investigate calcium-activated proteinases on CCTα degradation, cells were exposed to A23187, which stimulates calpain activity. Similar to Ox-LDL, the ionophore A23187 induced CCTα degradation (Fig. 4*C*). Calpain-mediated proteolysis in cells is tightly regulated by the availability of its endogenous inhibitor, calpastatin. When MLE cells were transfected with a plasmid encoding a calpastatin inhibitory domain fragment, the effects of Ox-LDL on CCTα degradation were reduced compared with cells transfected with a control plasmid (Fig. 4*D*). Further, overexpression of calpain in MLE cells induced CCTα degradation similar to calcium ionophore (Fig. 4*E*). These changes in CCTα protein levels were associated with coordinate changes in activity (Fig. 4, *F* and *G*). Finally, the effects of Ox-LDL were tested in calpain-deficient fibroblasts (26). Wild-type cells generally expressed lower levels of CCTα compared with calpain-deficient cells (Fig. 4*H*). Ox-LDL produced a 36 ± 5% decrease in CCTα levels in wild-type cells, whereas the particles decreased enzyme levels only by 16 ± 2% in cells lacking calpain (Fig. 4, *H* and *I*). Thus, calpain activated in response to exogenous oxidized lipoproteins triggers CCTα proteolysis and inhibition of surfactant PtdCho synthesis.

Ox-LDL Increases Calpain Expression

Low levels of constitutively expressed calpain transcripts were detected in lung epithelia. Ox-LDL induced M-calpain and μ-calpain mRNA nearly 5-fold and 3-fold, respectively, compared with control (Fig. 5*A*). These effects of Ox-LDL on calpain transcripts resulted in a coordinate increase in immunoreactive M-calpain and μ-calpain in cells after 24 h of Ox-LDL treatment (Fig. 5*B*).

Characterization of a CCTα Cleavage Product of Calpain

To localize calpain cleavage sites within the CCTα primary structure, we performed proteinase digestion of lysates after transfection of cells with truncated or internal deletion mutants of CCTα. The products of the reaction were then analyzed by immunoblotting using an antibody directed against epitopes (residues 164–176 (10)) within the CCTα catalytic domain (Fig. 6*A*). Calpain hydrolysis of lysates isolated from cells transfected with His-tagged full-length pCMV5-CCTα or the internal deletion mutant, His-tagged pCMV5-CCT$_{289}$, led to the appearance of one or more degradation bands. Specifically, a 26-kDa product (p26) was detected when full-length CCTα and pCMV5-CCT$_{289}$ constructs were expressed in cells and purified (to remove endogenous CCTα) prior to immunoblotting (Fig. 6*A*). Similar results with p26 were seen using the pCMV5-CCT$_{236}$ and pCMV5-CCT$_{314}$ constructs (data not shown). Long-term (>16 h) hydrolysis of CCTα resulted in the disappearance of this fragment and the emergence of faster migrating products (<24 kDa) as described previously (10). Thus, calpain hydrolysis of various CCTα mutants, all harboring the nuclear localization and catalytic

domains, resulted in the appearance of an identical 26-kDa product, suggesting that it resulted from two cleavages within a substrate spanning the amino terminus to residue 236 of CCTα.

To identify the amino-terminal cleavage site of CCTα by calpain, recombinant purified CCTα was reacted *in vitro* with M-calpain under optimal conditions (Fig. 6*B*). The reaction products were processed for Coomassie Blue staining and the digested bands submitted for NH_2-terminal sequencing. Reaction products from the initial calpain digestion were also processed for CCTα immunoblotting (Fig. 6*C*). Calpain hydrolysis of CCTα resulted in the appearance of prominent ~34- and ~26-kDa bands. Because the 34- and 26-kDa fragments comigrated in head-to-head studies with similar products reacting on immunoblots, these bands were sequenced. Analysis of the 34-kDa band was unsuccessful. Sequence analysis of the 26-kDa band revealed residues SAKVN corresponding to amino acids 5–9 of the NH_2-terminal region of CCTα (Fig. 6*D*).

To determine the carboxyl-terminal cleavage site, preliminary studies using matrix-assisted laser desorption ion mass spectrometric (MALDI-MS) analysis of p26 following a trypsin internal digest suggested a carboxyl-terminal cleavage site between residues 234 and 241 (Fig. 6*D*, data not shown). Together, these studies indicate that calpain produces at least two cleavages within CCTα with one cleavage very near the amino terminus. Based on molecular size estimates and MALDI-MS of p26, a second carboxyl-terminal cleavage site likely occurs near the catalytic membrane-binding hinge region, generating a fragment that presumably harbors the entire CCTα catalytic core.

Altered Calpain Sensitivity by CCTα Mutants

To further investigate calpain hydrolysis of CCTα, we generated a mutant where the amino-terminal calpain cleavage site was altered. We generated a second CCTα variant that harbored this amino-terminal mutation but also had residues Lys^{238}-Lys^{239}-Tyr^{240} mutated to Arg^{238}-Arg^{239}-Phe^{240} encompassing a region within the putative carboxyl-terminal cleavage site ($CCT\alpha_{Penta}$). After transfection of CHO cells with these mutant constructs, lysates were subjected to calpain hydrolysis and immunoblotting (Fig. 7*A*). Calpain treatment of expressed full-length CCTα (pCMV5-CCTα) or $CCT\alpha_{Penta}$ resulted in a decrease in the overall level of the 42-kDa expressed product. Unlike in MLE cells, hydrolysis of full-length CCTα in CHO cells led to the appearance of p26 and additional bands ranging in size from 20 to 30 kDa. Moreover, compared with proteinase treatment of full-length CCTα, hydrolysis of $CCT\alpha_{Penta}$ by calpain resulted in a significant decrease in the appearance of these faster migrating degradation products, and p26 was not detected (Fig. 7*A*, *double arrowhead*). Upon calpain treatment of $CCT\alpha_{SM}$, an amino-terminal mutant, no significant differences were displayed in the pattern of degradation products compared with the hydrolysis of expressed full-length CCTα (data not shown). Thus, mutagenesis of calpain cleavage sites within CCTα can significantly block proteinase activity *in vitro*.

To investigate proteinase resistance *in vivo*, the levels of 42-kDa product were analyzed after CCTα mutants were expressed in cells and were subsequently exposed to Ox-LDL (Fig. 7*B*). Vulnerability to Ox-LDL-induced proteolysis was significantly different among the individual CCTα mutants. Expression of full-length pCMV5-CCTα or $CCT\alpha_{SM}$ exhibited a 37 and 16% reduction in enzyme mass, respectively, in response to Ox-LDL compared with untreated control transfectants (Fig. 7*C*, $n = 3$). In contrast, expression of $CCT\alpha_{Penta}$ followed by Ox-LDL exposure resulted in enzyme levels comparable with those in untreated controls. Further, CCT activity for $CCT\alpha_{Penta}$ was significantly higher compared with other constructs after Ox-LDL treatment (Fig. 7*D*). Finally, we observed that cells transfected with $CCT\alpha_{Penta}$ restored the rates of choline incorporation into PtdCho similar to control levels, whereas expression of full-length CCTα or $CCT\alpha_{SM}$ exhibited a 57 and 29% reduction, respectively (Fig. 7*E*). Thus, cells transfected with the $CCT\alpha_{Penta}$ mutant were significantly less sensitive to the effects of

oxidized lipoproteins when compared with the sensitivity of full-length CCTαor the amino-terminal CCT mutant.

DISCUSSION

These studies have uncovered a previously unrecognized deleterious effect of pro-atherogenic lipoproteins on surfactant metabolism. This is the first demonstration that oxidized lipoprotein catabolism by alveolar epithelia suppresses surfactant PtdCho synthesis via calpain-mediated degradation of the rate-regulatory enzyme, CCTα. Moreover, these effects can be overcome by expression of proteinase-resistant enzyme mutants. Evidence supporting a role for calpain degradation of CCTα includes: (i) oxidized LDL stimulate calpain expression in alveolar cells resulting in increased CCTα turnover; (ii) the effects of oxidized LDL on CCTα degradation are reproduced by forced expression of calpain or exposure of cells to calcium ionophore; (iii) overexpression of calpastatin attenuates oxidized LDL degradation of CCTα; (iv) the effects of these modified lipoproteins on CCTα breakdown are reduced in calpain-deficient cells; and (v) purified calpain hydrolyzes recombinant CCTα specifically at the amino terminus and, most likely, near the catalytic membrane hinge region, generating a prominent 26-kDa fragment. Finally, degradation of CCTα was blocked *in vitro* and *in vivo* after expressing a CCTα mutant in cells in which proteinase-sensitive calpain sites had been altered. The biological relevance of these studies is that under the pathological conditions characterized by extravasation of circulating lipoproteins into the alveolus or during periods of prolonged hyperlipidemia, surfactant PtdCho synthesis might be significantly impaired as alveolar epithelial cells internalize oxidized particles. Because components of oxidized lipoproteins trigger a rise in cellular calcium (34), the activation of calpains may play an key role in controlling the life span of native CCTα. Thus, identification of proteolytic cleavage sites and cellular expression of functional CCTα mutants that are proteinase-resistant may ultimately prove useful in augmenting surfactant synthesis.

Oxidized LDL catabolism by alveolar epithelial cells resulted in significant inhibition of PtdCho synthesis by destabilizing CCTα protein. These results differ from those seen with native lipoproteins, where PtdCho synthesis is markedly stimulated as a result of post-translational CCTα activation (15,35). It remains unclear which components of Ox-LDL increase CCTα turnover. Oxidized phosphatidylcholines are unlikely factors because they stimulate CCT activity (36), although two other components, oxysterols or lysoPtdCho, may be more attractive candidates. In preliminary work, 22-hydroxycholesterol potently inhibits PtdCho synthesis,[2] and lysoPtdCho, a major lipoprotein component, triggers a burst in cytosolic calcium and calpain activation in bovine aortic endothelial cells (34). LysoPtdCho also competitively inhibits CCT activity and reduces PtdCho synthesis possibly via raft-dependent endocytosis (37,38). Further work is needed to determine whether these lipid components alone are necessary or sufficient to confer CCTα degradation by calpain.

Pharmacologic inhibitors have been used in some studies to demonstrate a link between calpain and protein degradation (34,39). Our prior work showing that tumor necrosis factor-α-induced degradation of CCTα is attenuated by a cysteine proteinase inhibitor is supportive, but conclusive evidence for the role of calpain in this process required complementary approaches (10). This was especially important because of inhibitor nonselectivity, and our data suggesting that CCTα degradation involved the ubiquitin-proteasome (Ref. 10 and Fig. 4). To assess the calpain system, we first observed a unique linkage between oxidized LDL, the induction of μ- and M-calpain, and the degradation of CCTα *in vivo*. The effects of calpain on CCTα breakdown were mimicked by A23187. Because calcium ionophore stimulates multiple intracellular events that could potentially modulate CCTα levels, we used genetic strategies to

[2]M. Aggasandian, J. Zhou, A. J. Ryan, and R. K. Mallampalli, unpublished data.

evaluate the role of calpain. Overexpression of rat M-calpain increased CCTα degradation, whereas expression of the specific endogenous calpain inhibitor, calpastatin, attenuated oxidized LDL-induced turnover of the enzyme. Overexpression of calpastatin inhibits both μ- and M-calpains. Because calcium levels in alveolar cells are generally in the nanomolar to micromolar range, μ-calpain might be the more physiologically relevant isoform regulating CCTα turnover in these cells (40,41). Finally, effects of oxidized LDL on CCTα breakdown were significantly reduced in cells lacking a key 28-kDa calpain subunit, *Capn4*, common to both μ- and M-calpain (26). In aggregate, these studies indicate that oxidized lipoprotein-induced CCTα catabolism is mediated, at least in part, by calcium-activated neutral proteinases.

Additional characterization of CCTα as a *bona fide* calpain substrate entailed the identification of calpain-specific cleavage sites. *In vitro* hydrolysis of CCTα and CCTα deletion mutants by calpain resulted in generation of a 26-kDa cleavage product. As seen with tumor necrosis factor-α, however, the detection of proteolytic fragments in cells after Ox-LDL treatment was inconsistent and was observed within a relatively short window of exposure (26–42 h) requiring prolonged exposure of immunoblots to autoradiographic film (data not shown) (10,42). Such fragments seen on our *in vitro* calpain digests are likely cleared rapidly in cells by the proteasome, thereby evading detection by conventional analysis (42,43). Expressional studies suggested that the 26-kDa breakdown product resulted from two cleavages, leading to a fragment that probably contained residues extending from the amino terminus through the CCTα catalytic core. NH_2-terminal sequencing of the 26-kDa product revealed that it was clipped just outside of the nuclear localization motif, a conserved region within the CCTα primary sequence. Cleavage within the CCTα nuclear localization sequence has recently been demonstrated by caspases (44). We were not able to pursue carboxyl-terminal analysis because of limited availability of purified CCTα, but this cleavage site most likely resides within the interface between the catalytic membrane-binding domains of the enzyme. This was supported by results derived from random mutagenesis within this region generating $CCT\alpha_{Penta}$, a mutant that contains both a modified amino-terminal calpain cleavage site and altered residues within the hinge region. Indeed, expression of $CCT\alpha_{Penta}$ in cells conferred partial calpain resistance *in vitro* and resulted in significant resistance to Ox-LDL-induced CCTα degradation *in vivo* (Fig. 7). Thus, the carboxyl-terminal clip likely occurs between residues 238 and 240 of CCTα. Further, the $CCT\alpha_{Penta}$ construct retained significant biologic activity despite Ox-LDL treatment (Fig. 7, *D* and *E*). Interestingly, calpain cleavage within domain hinge regions has been described for protein kinase C, resulting in the generation of a physiologically active fragment (45). The amino-terminal cleavage site of CCTα between Ser^5 and Ser^6 also resembles hydrolysis of protein kinase C-γ but contrasts with prior studies showing calpain selectivity for Tyr, Met, or Arg and hydrophobic residues flanking attack sites (45,46). Moreover, there is considerable variability for cleavage sites between different calpain substrates, suggesting that structural features such as enzyme conformation or accessibility might dictate CCT vulnerability to proteolysis (39). In this regard, the amino terminus of CCTα might be relatively exposed and thus hypersensitive to cleavage.

Further studies are required to address whether calpain hydrolysis of CCTα serves primarily as a regulatory role *versus* an initial degradative step in the overall processing of the enzyme for cellular elimination. With regard to a regulatory role, limited calpain proteolysis of protein kinase C generates a functional 51-kDa fragment (47), and calpain cleavage of the neuronal activator p35 generates a fragment that is dysregulatory (48). Similarly, CCTα degradation by calpains might result in the generation of transiently active intermediates that participate in PtdCho biosynthesis. In a more likely scenario, limited proteolysis of CCTα by calpain might simply destabilize the enzyme, making it susceptible to further degradation by the proteasome (49). Indeed, dual proteolysis pathways govern degradation of other regulatory proteins, and the proteasome partakes in CCTα turnover (10,42,50). The presence of a destabilizing NH_2 terminus with several internal lysine residues might direct CCTα for polyubiquitination prior

to proteasomal degradation. Data base analysis of CCTα(www.biu.icnet.uk/projects/pest/) also reveals the presence of a PEST sequence within the nuclear targeting domain that might confer a proteolytic signal for ubiquitin-proteasomal processing via enhanced binding to ubiquitin ligase (51).

In summary, this study reveals that Ox-LDL inhibits surfactant PtdCho synthesis by inducing calpain-mediated cleavage of CCTα within at least two specific-sites. By expressing a mutant CCTα where these proteinase-sensitive sites were altered, we successfully restored enzyme activity and PtdCho synthesis to levels comparable with control. We speculate that cellular expression of proteinase-resistant surfactant mutants might serve as a novel therapeutic approach to stimulate surfactant lipid synthesis in acute lung injury.

REFERENCES

1. Rooney SA. Am. Rev. Respir. Dis 1985;131:439–460. [PubMed: 2858175]
2. Kent C. Biochim. Biophys. Acta 1997;1348:79–90. [PubMed: 9370319]
3. Wang Y, Sweitzer TD, Weinhold PA, Kent C. J. Biol. Chem 1993;268:5899–5904. [PubMed: 8383679]
4. Ridsdale R, Tseu I, Wang J, Post M. J. Biol. Chem 2001;276:49148–49155. [PubMed: 11583989]
5. Yang W, Jackowski S. J. Biol. Chem 1995;270:16503–16506. [PubMed: 7622451]
6. Pelech SL, Pritchard PH, Brindley DN, Vance DE. J. Biol. Chem 1983;258:6782–6788. [PubMed: 6304057]
7. Feldman DA, Kovac CR, Dranginis PL, Weinhold PA. J. Biol. Chem 1978;253:4980–4986. [PubMed: 209024]
8. Bakovic M, Waite K, Tang W, Tabas I, Vance DE. Biochim. Biophys. Acta 1999;1438:147–165. [PubMed: 10216289]
9. Tessner TG, Rock CO, Kalmar GB, Cornell RB, Jackowski S. J. Biol. Chem 1991;266:16261–16264. [PubMed: 1653227]
10. Mallampalli RK, Ryan AJ, Salome RG, Jackowski S. J. Biol. Chem 2000;275:9699–9708. [PubMed: 10734122]
11. Groblewski GE, Wang Y, Ernst SA, Kent C, Williams JA. J. Biol. Chem 1995;270:1437–1442. [PubMed: 7836412]
12. Golfman LS, Bakovic M, Vance DE. J. Biol. Chem 2001;276:43688–43692. [PubMed: 11557772]
13. Lykidis A, Baburina I, Jackowski S. J. Biol. Chem 1999;274:26992–27001. [PubMed: 10480912]
14. Lykidis A, Jackson P, Jackowski S. Biochemistry 2001;40:494–503. [PubMed: 11148044]
15. Mallampalli RK, Salome RG, Bowen SL, Chappell DA. J. Clin. Invest 1997;99:2020–2029. [PubMed: 9109447]
16. Ryan AJ, Medh JD, McCoy DM, Salome RG, Mallampalli RK. Am. J. Physiol 2002;283:L310–L318.
17. Jialal I, Devaraj S. Clin. Chem 1996;42:498–506. [PubMed: 8605665]
18. Schunemann HJ, Muti P, Freudenheim JL, Armstrong D, Browne R, Klocke RA, Trevisan M. Am. J. Epidemiol 1997;146:939–948. [PubMed: 9400335]
19. Jobe AH, Ikegami M. Proc. Assoc. Am. Physicians 1998;110:489–495. [PubMed: 9824531]
20. Emmett M, Fowler AA, Hyers TM, Crowle AJ. Proc. Soc. Exp. Biol. Med 1987;184:83–91. [PubMed: 3797428]
21. Kolleck I, Schlame M, Fechner H, Looman AC, Wissel H, Rustow B. Free Radic. Biol. Med 1999;27:882–890. [PubMed: 10515593]
22. Chappell DA, Fry GL, Waknitz MA, Muhonen LE, Pladet MW. J. Biol. Chem 1993;268:25487–25493. [PubMed: 8244984]
23. Luche MM, Rock CO, Jackowski S. Arch. Biochem. Biophys 1993;301:114–118. [PubMed: 8382903]
24. Wang Y, Kent C. J. Biol. Chem 1995;270:18948–18952. [PubMed: 7642553]
25. Huang J, Forsberg NE. Proc. Natl. Acad. Sci. U. S. A 1998;95:12100–12105. [PubMed: 9770446]

26. Arthur JS, Elce JS, Hegadorn C, Williams K, Greer PA. Mol. Cell. Biol 2000;20:4474–4481. [PubMed: 10825211]
27. Esterbauer H, Gebicki J, Puhl H, Jurgens G. Free Radic. Biol. Med 1992;13:341–390. [PubMed: 1398217]
28. Longo CA, Tyler D, Mallampalli RK. Am. J. Respir. Cell Mol. Biol 1997;16:605–612. [PubMed: 9160843]
29. Balibrea-Cantero JL, Arias-Diaz J, Garcia C, Torres-Melero J, Simon C, Rodriguez JM, Vara E. Am. J. Respir. Crit. Care Med 1994;149:699–706. [PubMed: 8118639]
30. Bligh EG, Dyer WJ. Can. J. Biochem. Physiol 1959;37:911–917. [PubMed: 13671378]
31. Mallampalli RK, Salome RG, Spector AA. Am. J. Physiol 1994;267:L641–L648. [PubMed: 7810669]
32. Mallampalli RK, Mathur SN, Warnock LJ, Salome RG, Hunninghake GW, Field FJ. Biochem. J 1996;318:333–341. [PubMed: 8761490]
33. Rosner, BA. Fundamentals of Biostatistics. Belmont, CA: Wadsworth Publishing Co.; 1995. p. 314-318.
34. Chaudhuri P, Colles SM, Damron DS, Graham LM. Arterioscler. Thromb. Vasc. Biol 2003;23:218–223. [PubMed: 12588762]
35. Shiratori Y, Houweling M, Zha X, Tabas I. J. Biol. Chem 1995;270:29894–29903. [PubMed: 8530387]
36. Drobnies AE, van der Ende B, Thewalt JL, Cornell RB. Biochemistry 1999;38:15606–15614. [PubMed: 10569945]
37. Boggs KP, Rock CO, Jackowski S. J. Biol. Chem 1995;270:7757–7764. [PubMed: 7706325]
38. van der Luit AH, Budde M, Ruurs P, Verheij M, van Blitterswijk WJ. J. Biol. Chem 2002;277:39541–39547. [PubMed: 12183451]
39. Croall DE, DeMartino GN. Physiol. Rev 1991;71:813–847. [PubMed: 2057527]
40. Papen M, Wodopia R, Bartsch P, Mairbaurl H. Cell. Physiol. Biochem 2001;11:187–196. [PubMed: 11509826]
41. Isakson BE, Evans WH, Boitano S. Am. J. Physiol 2001;280:L221–L228.
42. Han Y, Weinman S, Boldogh I, Walker RK, Brasier AR. J. Biol. Chem 1999;274:787–794. [PubMed: 9873017]
43. Botbol V, Scornik OA. J. Biol. Chem 1983;258:1942–1949. [PubMed: 6822543]
44. Lagace TA, Miller JR, Ridgway ND. Mol. Cell. Biol 2002;22:4851–4862. [PubMed: 12052891]
45. Kishimoto A, Mikawa K, Hashimoto K, Yasuda I, Tanaka S, Tominaga M, Kuroda T, Nishizuka Y. J. Biol. Chem 1989;264:4088–4092. [PubMed: 2537303]
46. Sasaki T, Kikuchi T, Yumoto N, Yoshimura N, Murachi T. J. Biol. Chem 1984;259:12489–12494. [PubMed: 6092335]
47. Kishimoto A, Kajikawa N, Shiota M, Nishizuka Y. J. Biol. Chem 1983;258:1156–1164. [PubMed: 6296071]
48. Patzke H, Tsai LH. J. Biol. Chem 2002;277:8054–8060. [PubMed: 11784720]
49. Suzuki K, Imajoh S, Emori Y, Kawasaki H, Minami Y, Ohno S. Adv. Enzyme Regul 1988;27:153–169. [PubMed: 2854947]
50. Wang N, Chen WG, Linsel-Nitschke P, Martinez LO, Agerholm-Larsen B, Silver DL, Tall AR. J. Clin. Invest 2003;111:99–107. [PubMed: 12511593]
51. Roth AF, Sullivan DM, Davis NG. J. Cell Biol 1998;142:949–961. [PubMed: 9722608]

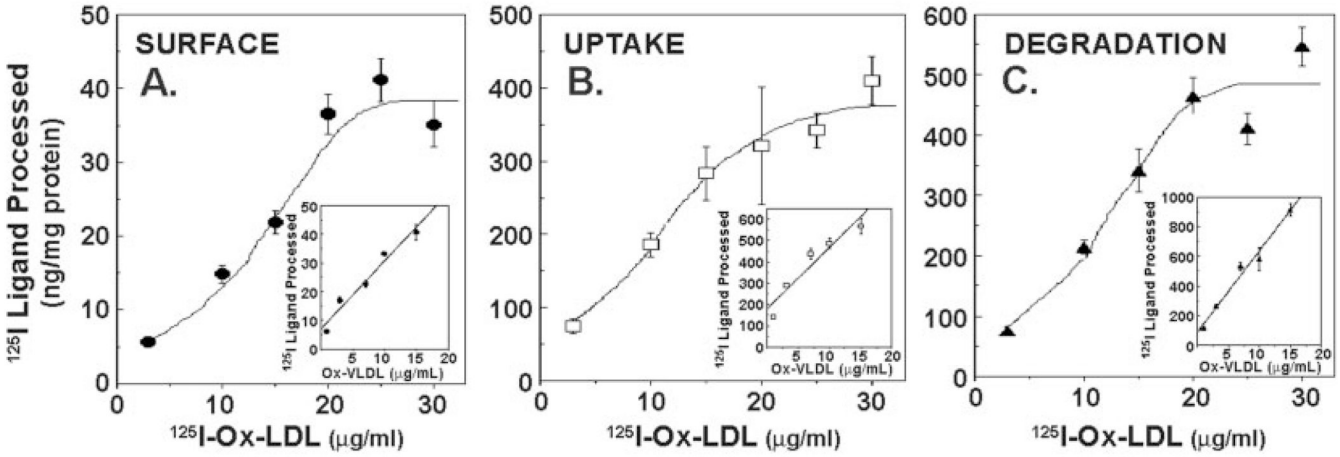

FIG. 1. Oxidized low density lipoprotein catabolism by alveolar epithelia

Confluent MLE cells were incubated with various amounts (3–30 μg/μl) of ^{125}I-Ox-LDL or ^{125}Ox-VLDL (*inset*) for 5 h at 37 °C. Steady-state levels of ligand surface binding (*A*), uptake (*B*), and degradation (*C*) were then determined.

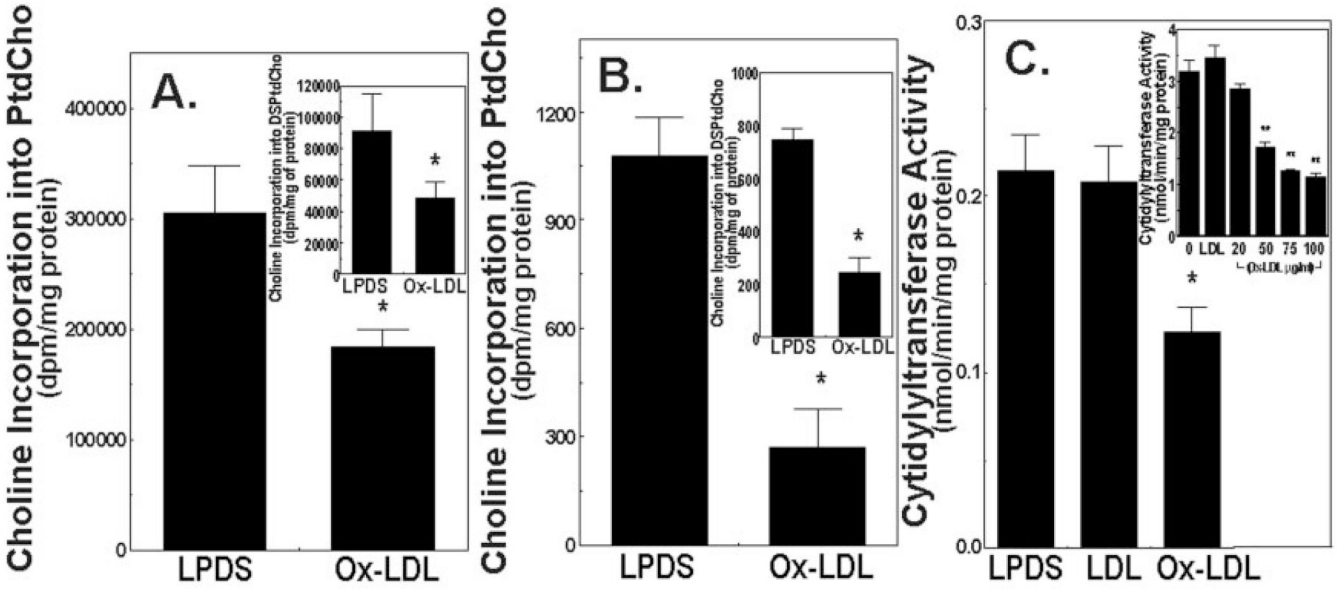

FIG. 2. Oxidized lipoproteins inhibit PtdCho biosynthesis

Primary rat type II cells (*A*) and MLE cells (*B*) were incubated for 24 or 48 h, respectively, in medium containing 10% LPDS alone or in combination with Ox-LDL (75 μg/ml). Cells were pulsed with [*methyl*-^{3}H]choline chloride, and choline incorporation into PtdCho or DSPtdCho (*inset*) was then measured. *C*, primary alveolar epithelia were incubated as described above with LPDS or LPDS with native LDL (75 μg/ml) or Ox-LDL (75 μg/ml) for 24 h. *Inset*, MLE cells were cultured for 48 h with LPDS, LPDS with LDL (75 μg/ml), or LPDS with Ox-LDL (20–100 μg/ml). Cells were analyzed for CCT activity. Results are mean ± S.E. from $n = 3$ experiments. *, $p < 0.05$ *versus* LPDS; **, $p < 0.01$ *versus* LPDS (○).

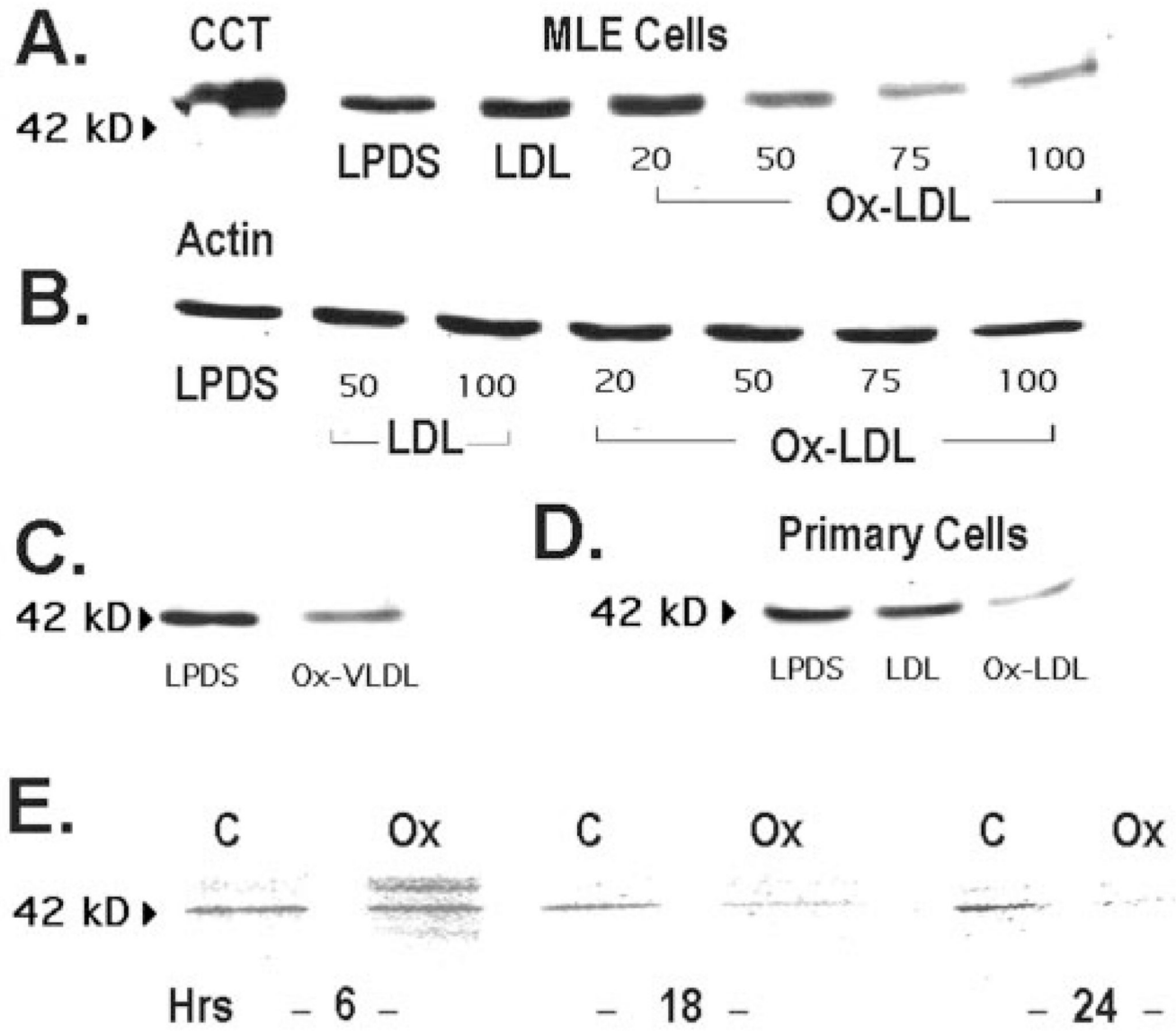

FIG. 3. Oxidized lipoproteins degrade CCTα protein

A, MLE cells were cultured in the presence of LPDS, LPDS with LDL (100 μg/ml), or various amounts of Ox-LDL (20–100 μg/ml) for 48 h, and CCTα protein levels were determined. The *leftmost lane* is the purified CCTα standard (2 μg). *B*, levels of β-actin were determined under conditions similar to those described in *A*. *C*, cells were incubated with LPDS or in combination with Ox-VLDL (100 μg/ml) for 48 h, and CCTα levels were determined. *D*, primary rat alveolar type II epithelial cells were incubated for 24 h with LPDS, LPDS plus LDL (*LDL*, 75 μg/ml), or LPDS plus Ox-LDL (*Ox-LDL*, 75 μg/ml), and CCTα protein levels were determined. All lanes in *panels A–D* contain equal amounts of total cellular protein. *E*, CCTα protein degradation in MLE cells was determined by pulsing cells with [^{35}S]methionine for 4 h; cells were rinsed and incubated with chase medium (10) for 6–24 h with or without 100 μg/ml Ox-LDL (*Ox*). Equal amounts of enzyme protein were immunoprecipitated with CCTα antibody. *A–D*, n = 4 separate studies; *E*, n = 2 studies.

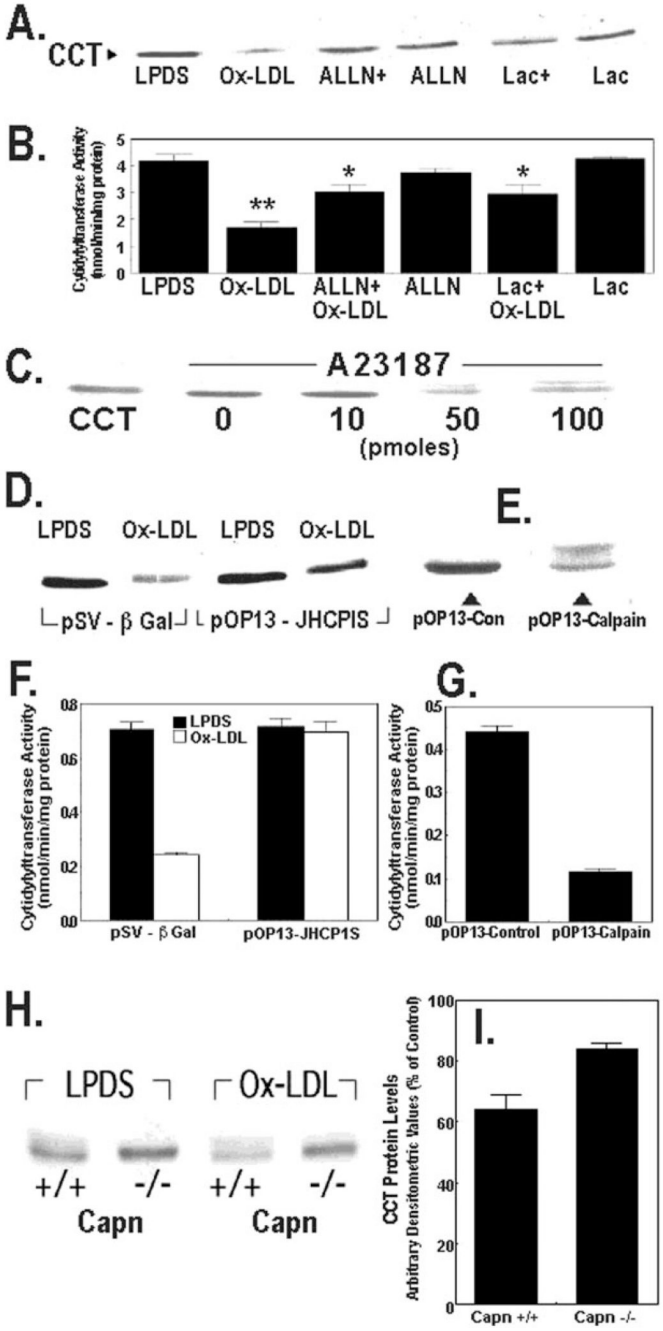

FIG. 4. Degradation of CCTα by oxidized LDL is mediated by calpain

A and *B*, MLE cells cultured in LPDS with or without oxidized LDL Ox-LDL (100 μg/ml) were pretreated with ALLN (40 μg/ml) or lactacystin (*Lac*) (5 μM) for 1 h alone or prior to exposure to Ox-LDL for 48 h. The levels of CCTα protein (*A*) or activity (*B*) were then assayed. *ALLN+*, ALLN plus Ox-LDL; *Lac+*, lactacystin plus Ox-LDL. **, $p < 0.01$ *versus* all groups; *, $p < 0.05$ *versus* LPDS, Ox-LDL, and Lac groups by ANOVA; $n = 3$ separate studies. *C*, cells were cultured in LPDS alone or with various amounts of A23187 for 18 h. Cells were then harvested for CCTα immunoblotting. The *leftmost lane* contains CCTα standard (2 μg). *D*, cells were transfected with a control plasmid, pSV-β-galactosidase (5 μg), or the calpastatin inhibitory domain fragment, pOP13-JHCPIS (5 μg), and allowed to recover for 24 h before

incubation with or without Ox-LDL (100 μg/ml) for 48 h. Cells were then harvested for CCTα immunoblotting. *E*, cells were transfected with a defective M-calpain control plasmid (5 μg) or a plasmid encoding M-calpain, pOP13-calpain (5 μg). Cells were processed for CCTα immunoblotting. *F* and *G*, CCT activity was determined in the cellular lysates from studies shown in *panels D* and *E*. *H* and *I*, calpain-deficient cells (*Capn* −/−) or wild-type controls (*Capn* +/+) were cultured for 48 h in LPDS with or without Ox-LDL (100 μg/ml). Cells were harvested for CCTα immunoblotting, and densitometric analysis of immunoblots was performed on the 42-kDa enzyme. *Panel I* represents the percent of CCTα protein detected in each cell type after Ox-LDL treatment relative to LPDS controls. All lanes in the individual panels were loaded with equal amounts of total cellular protein.

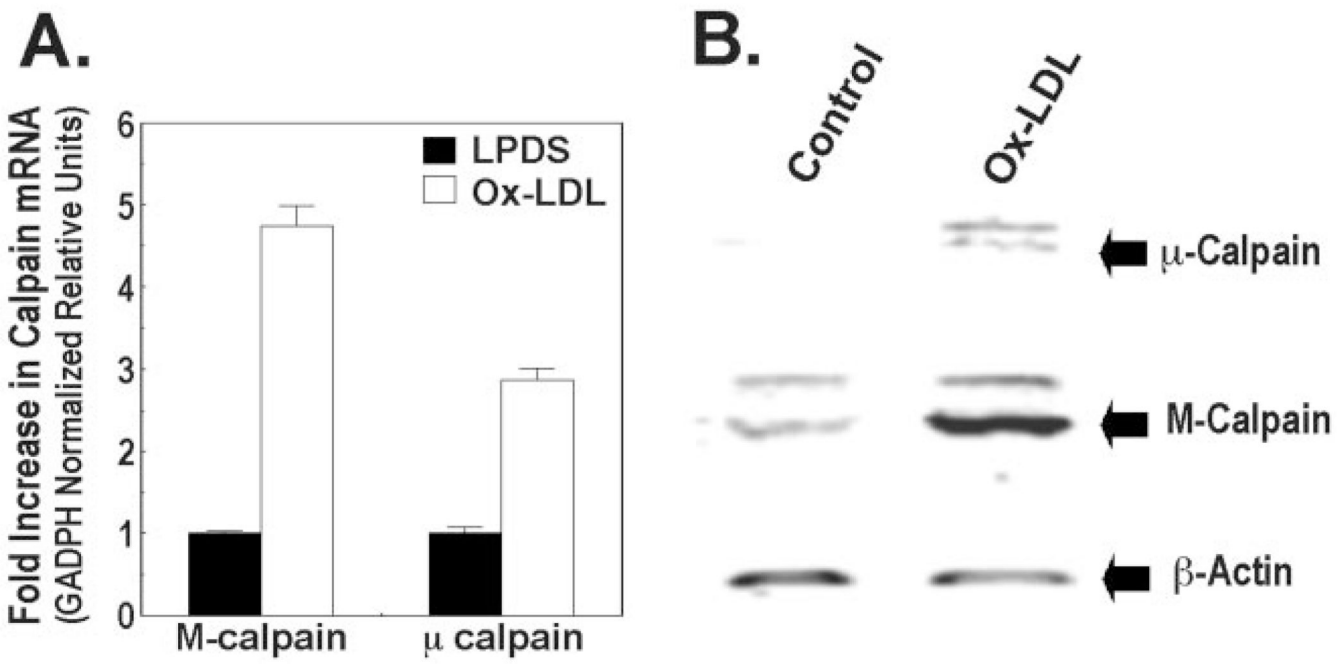

FIG. 5. Oxidized LDL increases calpain expression

A, MLE cells were cultured in LPDS with or without Ox-LDL (100 μg/ml) for 48 h, and total cellular RNA was harvested for analysis of M-calpain and μ-calpain by real-time PCR. Values are expressed as the mean ± S.E. of relative units, which were first normalized to murine glyceraldehyde-3-phosphate dehydrogenase (*GAPDH*). *B*, cells cultured in LPDS with or without Ox-LDL for 48 h were analyzed for levels of immunoreactive M-calpain and μ-calpain. Data are representative of three experiments.

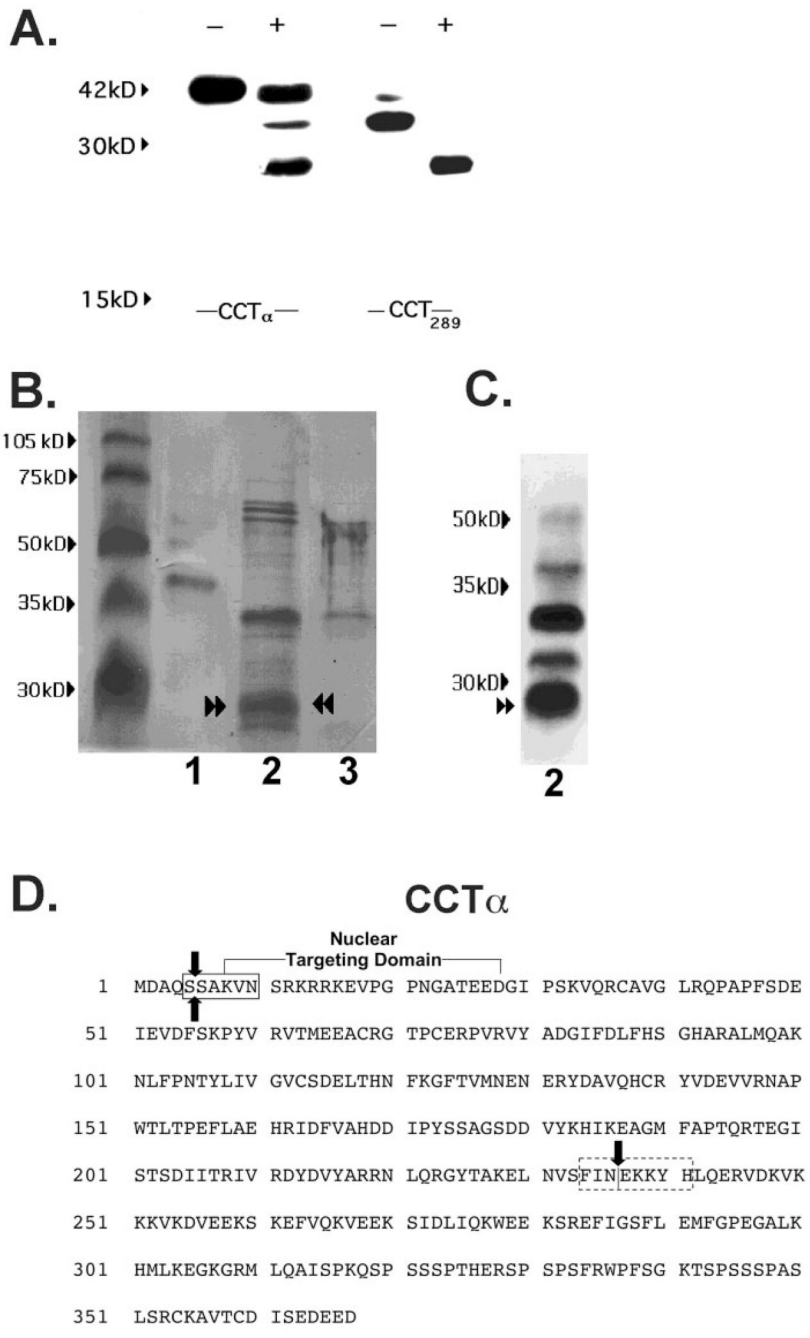

FIG. 6. *In vitro* digestion of CCTα by purified M-calpain

A, MLE cells were transfected with His-tagged full-length pCMV5-CCTα (*CCTα*) and the internal deletion mutant, His-tagged pCMV5-CCT_{289} (*CCT_{289}*), which lacks the membrane-binding domain. After a 24-h recovery period, lysates were harvested. Lysates were purified on a His-tagged column and treated without (−) or with (+) M-calpain (0.7 μg) for 30 min prior to SDS-PAGE and immunoblotting for CCTα. Data are representative of four separate studies. *B*, Coomassie Blue staining of CCTα cleavage products after calpain treatment. Recombinant purified CCTα alone (2 μg (*lane 1*), purified CCTα (25 μg) in combination with M-calpain (0.7 μg) (*lane 2*), or M-calpain alone (0.7 μg) (*lane 3*) were reacted *in vitro* for 30 min and the reaction products run on SDS-PAGE followed by transfer to Problot membranes for Coomassie

Blue staining. *C*, immunoblotting for CCTα cleavage products from proteolysis reactions described in *B*, *lane 2*, was performed. *Paired arrowsheads* represent an ~26-kDa CCTα degradation product that was submitted for NH_2-terminal sequencing. *D*, the primary sequence of CCTα showing the amino-terminal cleavage site outside of the nuclear targeting domain (*boxed* region) identified by NH_2-terminal sequencing of the 26-kDa calpain fragment (*paired arrows*). The *dotted box* indicates the putative carboxyl-terminal calpain cleavage region suggested by MALDI-MS. The *single vertical arrow* indicates the catalytic membrane-binding domain boundary.

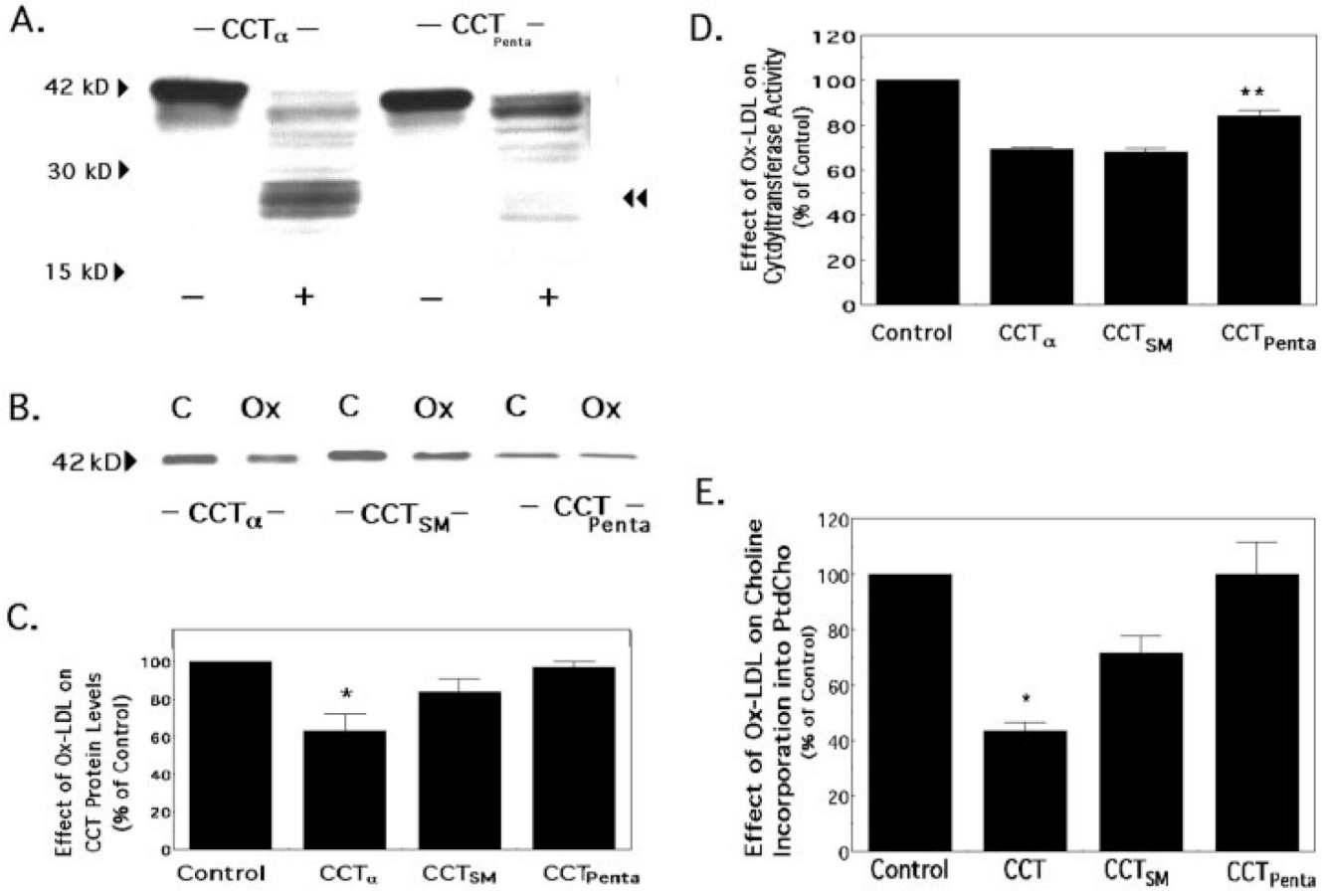

FIG. 7. Sensitivity of CCTα variants to M-calpain hydrolysis and Ox-LDL treatment

A, CHO cells were transfected with plasmids encoding full-length CCTα or a variant, $CCT\alpha_{Penta}$, where the amino-terminal calpain cleavage site was altered by mutation of Ser^5 and Ser^6 to Met, and residues Lys^{238}-Lys^{239}-Tyr^{240} were mutated to Arg^{238}-Arg^{239}-Phe^{240}. After cells were transfected, lysates were left untreated (−) or subjected to calpain hydrolysis (+) prior to immunoblotting, as described under "Experimental Procedures," to determine the proteolytic profile. The *double arrowhead* indicates the 26-kDa cleavage product. Each of the lanes on SDS-PAGE was loaded with 40 μg of total cellular protein. The results are representative of three separate studies. *B*, cells were transfected with plasmids encoding full-length CCTα, $CCT\alpha_{SM}$, when the amino-terminal calpain cleavage site alone was altered (Ser^5 and Ser^6 were mutated to Met), or $CCT\alpha_{Penta}$, when residues within both the amino-terminal and putative carboxyl-terminal calpain cleavage sites were mutated. Cells were subsequently exposed to LPDS alone (*C*, control) or LPDS in combination with Ox-LDL (*Ox*) (100 μg/ml) for 48 h and then harvested for CCTα immunoblotting. Each lane on SDS-PAGE was loaded with equal amounts of total cellular protein. *C*, densitometric analysis of immunoblots was performed on the 42-kDa protein. *Panel C* represents the percent of CCTα protein detected in cells in response to Ox-LDL treatment relative to untreated control cells after transfection of each individual plasmid. *D* and *E*, CCT activity (*D*) and [*methyl*-^{3}H]choline incorporation into PtdCho (*E*) were assayed as described in *B*. The data represent the percent of either CCTα activity (*D*) or choline incorporation into PtdCho (*E*) detected in cells in response to Ox-LDL treatment relative to untreated control cells after transfection of each individual plasmid. The results are representative of three separate studies for *B*; $n = 4$ for the experimental panels (*C* and *D*). *, $p < 0.05$ for percent reduction in response to Ox-LDL for

the full-length CCTα construct *versus* either control or percent reduction in response to Ox-LDL for the $CCT\alpha_{Penta}$ construct by ANOVA. **, $p < 0.05$ for percent reduction in response to Ox-LDL for the $CCT\alpha_{Penta}$ construct *versus* percent reduction in response to Ox-LDL for either the full-length CCTα construct or the $CCT\alpha_{SM}$ construct by ANOVA.